ON DISCRETE CONSTANT MEAN CURVATURE SURFACES

CHRISTIAN MÜLLER

Abstract. Recently a curvature theory for polyhedral surfaces has been established which associates with each face a mean curvature value computed from areas and mixed areas of that face and its corresponding Gaussian image face. Therefore a study of constant mean curvature (cmc) surfaces requires studying pairs of polygons with some constant non-vanishing value of the discrete mean curvature for all faces. We focus on meshes where all faces are planar quadrilaterals or planar hexagons. We show an incidence geometric characterization of a pair of parallel quadrilaterals having a discrete mean curvature value of -1. This characterization yields an integrability condition for a mesh being a Gaussian image mesh of a discrete cmc surface. Thus we can use these geometric results for the construction of discrete cmc surfaces. In the special case where all faces have a circumcircle we establish a discrete Weierstrass type representation for discrete cmc surfaces.

Contents

1. Introduction and Preliminaries

A discrete constant mean curvature surface, discrete cmc surface for short, is a discrete surface, i.e., a mesh, where an appropriate notion of a discrete mean curvature is constant on the entire mesh. In this way, discrete cmc surfaces discretize their counterparts in classical differential geometry, the smooth cmc surfaces. The study of surfaces of constant mean curvature is interesting from a purely mathematical viewpoint but it is also motivated from physics namely from the interest in the geometric shape of soap films. There are two different situations which need to be considered separately. First, the soap films which occur having the same pressure on both sides of the film corresponds to vanishing mean curvature. Second, if we have constant, but different, pressures on

2010 *Mathematics Subject Classification.* 52C99, 53A10, 53A40, 51A15.

Key words and phrases. discrete differential geometry, discrete curvatures, discrete cmc surfaces, discrete Weierstrass representation, oriented mixed area, geometric configurations.

both sides then the resulting soap film represents a surface with some non-vanishing constant mean curvature. In our paper we will focus on the later case.

Smooth cmc surfaces have been investigated now for a long time and the research in this area is far away from being complete. One question which stimulated research in this field was raised by H. Hopf who conjectured that the only closed, compact cmc surface in $\mathbb{R}^3$ is the sphere. H. Wente [21] however, showed the existence of cmc surfaces which are topologically equivalent to a torus, the now called Wente tori. U. Pinkall and I. Sterling [15] classified and constructed all cmc tori. We will generate an example of a discretized version of a Wente torus in Paragraph 6.4.

Our study of discrete cmc surfaces is located in the rising field of *discrete differential geometry*. This theory tries to discretize objects, notions, equations, and methods from classical differential geometry. A first approach in this direction was made by R. Sauer in his book 'Differenzengeometrie' [17]. A modern approach is the manuscript 'Discrete Differential Geometry: Integrable Structure' by A.I. Bobenko and Yu.B. Suris [4].

Different but equivalent characterizations of properties or notions in smooth differential geometry, such as the mean curvature for example, can be discretized in various different ways. The resulting discretizations need no longer be equivalent or are equivalent to only some other discretizations. In our special case we take over the definition of the discrete mean curvature which appears in the recently discovered curvature theory for polyhedral surfaces by A.I. Bobenko et al. [3]. The discrete curvature notions there are assigned to the faces of a mesh with respect to an edge-wise parallel mesh which is considered as a discrete Gaussian image.

1.1. **Basic notations.** In the present paper, we focus on meshes $\mathcal{M}$ whose faces are planar polygons. In other words, we are concerned with polyhedral surfaces. Each face F is an m-gon ($m \geq 3$) and can be described by an ordered list of vertices, say $F = (f_0, f_1, \ldots, f_{m-1})$, such that two vertices with succeeding indices, f_i and f_{i+1}, are connected by an edge. For an m-gon we will always take indices modulo m. The first forward difference operator will be denoted by $\delta f_i = f_{i+1} - f_i$.

1.2. **Quad-graphs.** For the most part of our work, we are interested in the local theory of quadrilateral meshes, i.e., meshes where all faces are planar quadrilaterals. Thus, the underlying graph $\mathcal{G}$ which represents the combinatorics of the mesh is, at least locally, the cell decomposition of an open disc whose faces are quadrilaterals. $\mathcal{G}$ is therefore called a *quad-graph*. The generic example of a quad-graph would be the $\mathbb{Z}^2$ grid or a part of it. A more elaborate example is shown in Figure 1.

1.3. **Koenigs meshes and Christoffel duality.** In the special setting of planar quadrilateral meshes there exists a subclass of meshes namely the so called *discrete Koenigs nets* or *Keonigs meshes*. We recall the definition of Koenigs meshes by following [4, Section 2.3]. A Koenigs mesh $\mathcal{M}$ is a mesh which has the combinatorics of a quad-graph $\mathcal{G}$ and which admits dualization. This means that there exists a real-valued function $\nu : V(\mathcal{G}) \to \mathbb{R} \setminus 0$ defined on the vertices $V(\mathcal{G})$ of the graph $\mathcal{G}$ (or, defined on the vertices $V(\mathcal{M})$, which of course is the same) such that $\nu_2 : \nu_0 = (M - f_2) : (M - f_0)$ and $\nu_3 : \nu_1 = (M - f_3) : (M - f_1)$, where M is the intersection point of the diagonals of the quadrilateral $F = (f_0, \ldots, f_3)$, and where ν_i is the function value of ν at

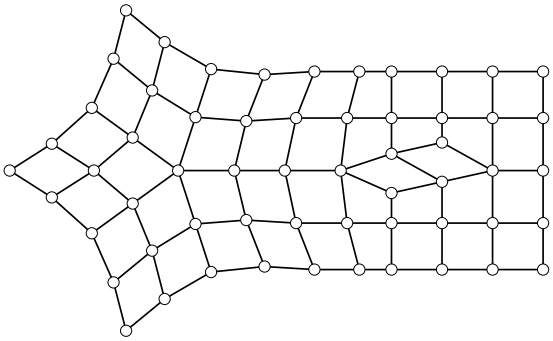

FIGURE 1. Illustration of a quad-graph with non $\mathbb{Z}^2$ combinatorics. Each face is a quadrilateral. Apart from the border this graph has vertices with valence three, four, and five.

the vertex f_i. Then, for each quadrilateral $F = (f_0, \dots, f_3)$ there exists a quadrilateral $F^* = (f_0^*, \dots, f_3^*)$ with

$$\delta f_i^* = \frac{\delta f_i}{\nu_i \nu_{i+1}}. \tag{1}$$

A mesh $\mathcal{M}^*$ where each face F^* is dual to the corresponding face F of a Koenigs mesh $\mathcal{M}$ with vertices f in the described way is called a *Christoffel dual* Koenigs mesh. If the starting mesh $\mathcal{M}$ approximates a sphere then the Christoffel dual mesh $\mathcal{M}^*$ represents a *discrete minimal surface*, see e.g., [1, 2]. It should be mentioned here that this is one of many possible definitions for an object called 'discrete minimal surface'. However, as it turns out, discrete minimal surfaces in the 'Christoffel dual' sense have vanishing discrete mean curvature in the setting of the discrete curvature theory [3] which we will present in Paragraph 1.5.

1.4. **Oriented mixed area.** In our discretization we are dealing with polyhedral surfaces and a discrete mean curvature notion coming from Steiner's formula. The smooth Steiner formula

$$\operatorname{area}(f^d) = \int_U (1 - 2dH + d^2K)\, d\mathbf{o}.$$

measures the area of the offset surface f^d of f at offset distance d. It is the surface integral over the parameter domain U where H and K are the mean and Gaussian curvature of f, respectively. Following [3] we will consider a discretization of Steiner's formula to obtain a discrete curvature notions. Suffice it to say here that for our discretization of the mean curvature the notion of planar parallel polygons plays an important role. Two planar m-gons $F = (f_0, \dots, f_{m-1})$ and $S = (s_0, \dots, s_{m-1})$ (with vertices f_i, $s_i \in \mathbb{R}^3$) are said to be *parallel* if all corresponding edges are parallel (i.e., $f_i - f_{i-1}$ and $s_i - s_{i-1}$ are linearly dependent; indices are taken modulo m). We can see right away that parallel polygons always lie in parallel planes.

This notion of parallel m-gons leads to a vector space in the following sense. We take a nondegenerate m-gon F, i.e., all edges have non-vanishing lengths, and consider the set $\mathcal{P}(F) := \{S \mid S \text{ is parallel to } F\}$. We immediately see that $\mathcal{P}(F)$ is a vector space

with vertex-wise addition and scalar multiplication

$$F + S := (f_0 + s_0, \dots, f_{m-1} + s_{m-1}) \quad \text{and} \quad \lambda F := (\lambda f_0, \dots, \lambda f_{m-1}).$$

As one verifies easily, this vector space $\mathcal{P}(F)$ has dimension $m + 1$. The functional to measure the oriented area of a planar polygon F is a discrete version of Leibnitz' sector formula

$$\operatorname{area}(F) = \frac{1}{2} \sum\nolimits_{i=0}^{m-1} \det(f_i, f_{i+1}, n),$$

where n is a unit normal vector of the supporting plane of F. This area functional, which is a quadratic form, induces a symmetric bilinear form

$$\operatorname{area}(F, S) := \frac{1}{4} \sum\nolimits_{i=0}^{m-1} \det(f_i, s_{i+1}, n) + \det(s_i, f_{i+1}, n),$$

for parallel m-gons F and S. This bilinear form is called *oriented mixed area* of two parallel m-gons F and S. This notion of the oriented mixed area first appeared in [16] and generalizes the classical mixed area that appears in the formula for the area of the Minkowski sum of two convex sets in $\mathbb{R}^2$. Following [13, Lemma 3] we obtain

$$4 \operatorname{area}(F, S) = \sum\nolimits_{i=0}^{m-1} \det(f_i, s_{i+1} - s_{i-1}, n) = \sum\nolimits_{i=0}^{m-1} \det(s_i, f_{i+1} - f_{i-1}, n). \tag{2}$$

We immediately see that the mixed area is invariant under translations of F and S as well as under orientation preserving isometries applied to both polygons at the same time. Therefore, w.l.o.g. we can always assume F and S to be contained in $\mathbb{R}^2$.

1.5. **Discrete mean curvature.** For the discretization of the mean curvature we follow [3, 16]. This discretization of the mean (and Gaussian) curvature appears the first time in the setting of circular meshes in [18, 19]. Their idea is to discretize Steiner's formula for the surface area of offset surfaces.

To discretize Steiner's formula one has to define an appropriate discrete offset surface for polyhedral surfaces. Different types of offsets may lead to different notions of curvatures. In our setting offset meshes are parallel meshes with some constant distance which has to be specified in more detail. A pair of *parallel meshes* consists of two meshes which have the same combinatorics and which have the property that corresponding faces are parallel. This immediately implies that all corresponding edges are parallel too. A special subclass of pairs of parallel meshes consists of the so called offset meshes. For the constant distance there are three common versions. The vertex [edge, face] offsets which means that the distances d between corresponding vertices [edges, faces] are constant. We have to note here that not all meshes possess these types of offsets. For the existence of vertex offsets, which depends also on the topology of the mesh, see e.g., [11].

Let us consider a mesh $\mathcal{M}$ and a vertex [edge, face] offset $\mathcal{M}^d$ at distance d. It is easy to see that as we subtract corresponding vertices of $\mathcal{M}$ and $\mathcal{M}^d$ and divide those by the distance d, we obtain the new planar mesh $\sigma(\mathcal{M}) := (\mathcal{M}^d - \mathcal{M})/d$. As one verifies immediately, $\sigma(\mathcal{M})$ is inscribed [midscribed, circumscribed] to the unit sphere $\mathbb{S}^2$. *Inscribed* means that the vertices lie in $\mathbb{S}^2$, *midscribed* means that the edges are tangent to $\mathbb{S}^2$, and *circumscribed* means that the faces are tangent to $\mathbb{S}^2$. It is therefore natural to see $\sigma(\mathcal{M})$ as a *discrete Gaussian image* of the discrete surface $\mathcal{M}$. On the other hand we can describe offset meshes $\mathcal{M}^d$ by the use of the Gaussian image

$$\mathcal{M}^d = \mathcal{M} + d\,\sigma(\mathcal{M}).$$

The existence of offset meshes of the described three types is equivalent to the existence of a Gaussian image mesh with the mentioned properties. For more details on this see e.g., [11, 16].

The discrete Steiner formula measures the surface area of offset meshes $\mathcal{M}^d$. We compare it with its smooth counterpart:

$$\operatorname{area}(\mathcal{M}^d) = \sum_{\text{Faces } F} (1 - 2dH_F + d^2 K_F) \operatorname{area}(F) \qquad \operatorname{area}(f^d) = \int_U (1 - 2dH + d^2 K)\, d\mathbf{o}.$$

A straightforward computation shows (for details see [3, 16]) that the coefficients H_F and K_F are given by

$$H_F = -\frac{\operatorname{area}(F, \sigma(F))}{\operatorname{area}(F)} \quad \text{and} \quad K_F = \frac{\operatorname{area}(\sigma(F))}{\operatorname{area}(F)}, \tag{3}$$

where $\sigma(F)$ is the corresponding face to F on the discrete Gaussian image mesh $\sigma(\mathcal{M})$. The notions H_F and K_F are called *discrete mean curvature* and *discrete Gaussian curvature*, respectively. We would like to note that in this setting the discrete curvatures correspond to faces in contrast to other definitions where they are corresponding to vertices (see e.g., [14]) or edges (see e.g., [20]). It is further important to remark that this definition only makes sense for meshes whose faces have more then three edges (except possibly for some isolated faces) because there are no nontrivial offsets of triangular meshes.

1.6. **Discrete constant mean curvature surfaces.** Equation (3) represents a discrete mean curvature notion and a discrete Gaussian curvature notion for polyhedral surfaces $\mathcal{M}$. This definition does not only depend on the mesh $\mathcal{M}$ alone but also on its Gaussian image $\sigma(\mathcal{M})$. Different Gaussian images belonging to the same mesh $\mathcal{M}$ lead to different values of the mean curvature. For example let us consider a mesh $\mathcal{M}$ with the combinatorics of a cell decomposition of a disc. Consequently, in the vertex offset case there exists a two parameter family of possible Gaussian images of $\mathcal{M}$. However, for meshes $\mathcal{M}$ which represent surfaces with a more complicated topology than a disc not even the existence of at least one suitable Gaussian image mesh is guaranteed. For more details see [11, 16].

In order to find *discrete constant mean curvature surfaces*, or shorter *discrete cmc* surfaces, we are looking for a pair of parallel meshes, namely $\mathcal{M}$ together with a suitable Gaussian image $\sigma(\mathcal{M})$, such that the discrete mean curvature H_F from (3) takes some constant value H for all faces F of the mesh $\mathcal{M}$.

In smooth differential geometry one distinguishes two types of cmc surfaces. Those with vanishing mean curvature ($H = 0$), which are the *minimal surfaces* and all the others with non-vanishing constant mean curvature ($H = \text{const.} \neq 0$). Some authors use the term 'cmc surfaces' just for the latter as we will do in the present paper. Different nonzero values of H do not require separate investigations since a scaling of the surface by a factor $\lambda \neq 0$ changes the mean curvature by the constant factor $1/\lambda$. I.e., it suffices to study cmc surfaces with $H = -1$, which is what we are going to do later. This scaling property carries over to the discrete setting as one verifies easily

$$H_{\lambda F} = -\frac{\operatorname{area}(\lambda F, \sigma(\lambda F))}{\operatorname{area}(\lambda F)} = -\frac{\lambda \operatorname{area}(F, \sigma(F))}{\lambda^2 \operatorname{area}(F)} = \frac{1}{\lambda} H_F, \tag{4}$$

since $\sigma(\lambda F) = \sigma(F)$.

Discrete minimal surfaces are characterized, in our setting, by vanishing mixed area of all faces of $\mathcal{M}$ with their corresponding faces of $\sigma(\mathcal{M})$, i.e., $\text{area}(F, \sigma(F)) = 0$ for all faces F of $\mathcal{M}$. They have been investigated in [3, 13, 16]. It turns out that discrete minimal surfaces generated via the approach using the discrete Christoffel dual construction (see Paragraph 1.3) have vanishing discrete mean curvature in the sense of (3) too.

We now turn to our main topic, the discrete cmc surfaces. Because of the bilinearity of the mixed area and the fact that $\text{area}(F) = \text{area}(F, F)$ we obtain:

$$H_F = -\frac{\text{area}(F, \sigma(F))}{\text{area}(F)} \quad \Longleftrightarrow \quad \text{area}(F, F + \frac{1}{H_F}\sigma(F)) = 0.$$

As indicated before, we are interested in discrete cmc surfaces with $H_F = -1$, i.e., we are looking for a mesh $\mathcal{M}$ with a suitable corresponding Gaussian image mesh $\sigma(\mathcal{M})$ such that

$$\text{area}(F, F - \sigma(F)) = 0 \tag{5}$$

holds for all faces F of $\mathcal{M}$. We will pay special attention to the cases where all faces (except maybe some isolated faces) are quadrilaterals or hexagons.

In the quadrilateral mesh case we have a connection to the Christoffel dual transformation. A Koenigs mesh $\mathcal{M}$ is cmc if and only if the offset mesh $\mathcal{M} - \sigma(\mathcal{M})$ equals $\mathcal{M}^*$, the Christoffel dual of $\mathcal{M}$. I.e., in terms of vertices: Let $F = (f_0, \dots, f_3)$, $F^* = (f_0^*, \dots, f_3^*)$, and $\sigma(F) = (s_0, \dots, s_3)$. Then $H_F = -1$ if and only if there exists a real-valued function $\nu : V(\mathcal{M}) \to \mathbb{R} \setminus 0$ defined on the vertices such that $\delta f_i - \delta s_i = \delta f_i^* = \frac{1}{\nu_i \nu_{i+1}} \delta f_i$ and therefore

$$\delta s_i = \frac{\nu_i \nu_{i+1} - 1}{\nu_i \nu_{i+1}} \delta f_i. \tag{6}$$

In conclusion, with Equation (6) we obtain a difference equation for a pair of meshes where f_i are the vertices of a discrete cmc surface with respect to the Gaussian image mesh with vertices s_i. For details see [4, Theorem 4.49].

2. Pairs of parallel polygons with $H_F = -1$

We have studied incidence geometric characterizations of pairs of parallel polygons F and $\sigma(F)$ in [13] to obtain discrete minimal surfaces. I.e., we investigated properties for $\text{area}(F, \sigma(F)) = 0$ which led to a recursive formula with a geometric interpretation. It turned out that we obtain such incidence geometric characterizations for pairs of polygons with an arbitrary number of vertices.

In order to find discrete cmc surfaces (with discrete mean curvature $H_F = -1$ for all faces) we are here concerned with Equation (5). I.e., the characterizing equation is $\text{area}(F, F - \sigma(F)) = 0$ which is equivalent to $H_F = -1$. Unfortunately, we cannot give an incidence geometric characterization for two parallel m-gons F and S with $m > 6$ but only for quadrilaterals and hexagons. For even $m > 6$ we have a sufficient but not necessary condition. Before we state our characterizations we have to make some preparations.

2.1. **The derived polygons.** We are aiming at an incidence geometric characterization of $\operatorname{area}(F, F-\sigma(F))=0$. As it turns out we are going to need some diagonals and lines parallel to diagonals of F and $\sigma(F)$ which leads us to the definition of so called derived polygons. We consider parallel polygons $F=(f_0,\dots,f_{m-1})$ and $S=(s_0,\dots,s_{m-1})$ with an even number m of vertices. In all our formulas we take indices modulo m. For the following constructions of the derived polygons we need one further condition to be fulfilled: Two successive 'diagonals' of F shall not be parallel, i.e., f_i-f_{i-2} and f_i-f_{i+2} are assumed to be linearly independent. We drop this condition for $m=4$ because otherwise we could not assign derived polygons to quadrilaterals. However, in this case the derived polygons will degenerate.

We call the following three polygons $F^*=(f_0^*,\dots,f_{m/2-1}^*)$, $\tilde{F}^*=(\tilde{f}_0^*,\dots,\tilde{f}_{m/2-1}^*)$, and $S^*=(s_0^*,\dots,s_{m/2-1}^*)$ *derived polygons* if

$$\begin{aligned} f_i^* &= f_{2i},\\ \tilde{f}_i^* &= (f_{2i-1}+[f_{2i-2}-f_{2i}])\cap(f_{2i+1}+[f_{2i}-f_{2i+2}]),\\ s_i^* &= (s_{2i-1}+[f_{2i-2}-f_{2i}])\cap(s_{2i+1}+[f_{2i}-f_{2i+2}]), \end{aligned}$$

holds. $[v]$ denotes the 1-dimensional linear subspace of a nonzero vector v. For an illustration of the derived polygons see Figure 2. Note that all three derived polygons F^*, $\tilde{F}^*$, and S^* are pairwise parallel polygons. The choice of the indices of the vertices to obtain the derived polygons is not significant and works just as well for the index shift $i\to i+1$. In that case we will denote the derived polygons by F^{**}, $\tilde{F}^{**}$, and S^{**} instead. It will be clear that all statements which hold for the derived polygons with ' * ' also hold for those with ' ** '.

In the quadrilateral case (i.e., $m=4$) the derived polygons degenerate. F^* is a two-sided polygon whereas $\tilde{F}^*$ and S^* consist of two parallel lines as illustrated by Figure 2 (right).

The relation between the mixed area of F and S and their derived polygons F^* and S^* is the content of the following theorem. For a proof see [13, Theorem 6].

THEOREM 1. *Let F and S be a pair of parallel polygons with an even number of vertices, and let F^*, S^*, F^{**}, and S^{**} be the derived polygons. Then the oriented mixed area is the same for all three pairs:* $\operatorname{area}(F,S)=\operatorname{area}(F^*,S^*)=\operatorname{area}(F^{**},S^{**})$.

2.2. **Pairs of parallel polygons with $H_F=-1$.** The following theorem describes a sufficient geometric condition for $H_F=-1$. As we have seen before (cf. Equation (5)) $H_F=-1$ is equivalent to $\operatorname{area}(F,F-\sigma(F))=0$. Since the following theorems are not depending in any way on $\sigma(F)$ being a polygon of a Gaussian image of some mesh but rather on the fact that $\sigma(F)$ is a polygon parallel to F, we will replace $\sigma(F)$ by S. Nonetheless, we will use the abbreviation $H_F=-1$ for $\operatorname{area}(F,F-S)=0$ which is coherent with the motivation of this work.

THEOREM 2. *Let $F=(f_0,\dots,f_{m-1})$ and $S=(s_0,\dots,s_{m-1})$ be two parallel m-gons, where m is even, such that the derived polygons F^*, $\tilde{F}^*$ and S^* exist. Then $H_F=-1$ if S^* and $\tilde{F}^*$ are equal up to translation.*

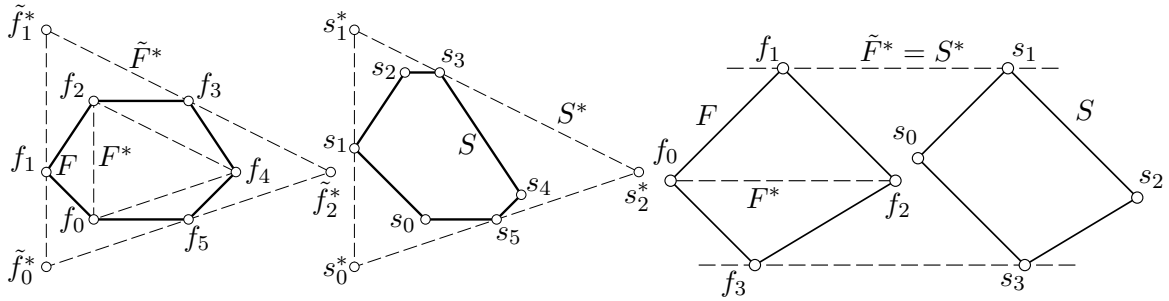

FIGURE 2. *Left:* A pair of parallel hexagons F and S such that $H_F = -1$. The derived polygons $\tilde{F}^*$ and S^* are equal up to translation (see Theorem 3). *Right:* A pair of parallel quadrilaterals F and S such that $H_F = -1$ (see Theorem 4). The derived polygon F^* of a quadrilateral consists just of the diagonal of F. $\tilde{F}^*$ and S^* degenerates to a pair of parallel lines.

Proof. We have

$$\operatorname{area}(F, S) = \operatorname{area}(F^*, S^*) = \operatorname{area}(F^*, \tilde{F}^*) = \operatorname{area}(F, F).$$

For the first and last equality we use Theorem 1. For the second equality w.l.o.g. we can use $S^* = \tilde{F}^*$ from the assumptions since translations leave the mixed area invariant. The third equality follows again from Theorem 1, since replacing S by F in Theorem 1 implies replacing S^* by $\tilde{F}^*$. Bilinearity of $\operatorname{area}(\cdot\ ,\cdot)$ yields $\operatorname{area}(F, F - S) = 0$ and therefore $H_F = -1$. □

One verifies easily by simple examples that the condition in Theorem 2, i.e., that the two derived polygons S^* and $\tilde{F}^*$ are equal, is not necessary for $H_F = -1$. However, for quadrilaterals and hexagons we do have a geometric 'if and only if' characterization.

THEOREM 3. *Let $F = (f_0, \dots, f_5)$ and $S = (s_0, \dots, s_5)$ be two parallel hexagons such that the derived polygons F^*, $\tilde{F}^*$ and S^* exist (see Figure 2 left). Then $H_F = -1$ if and only if S^* and $\tilde{F}^*$ are equal up to translation.*

Proof. Theorem 2 yields $H_F = -1$ if $\tilde{F}^*$ and S^* are equal up to translation. Thus, it remains to derive equality of $\tilde{F}^*$ and S^* up to translation from $H_F = -1$. Bilinearity of $\operatorname{area}(\cdot\ ,\cdot)$ yields $H_F = -1 \Leftrightarrow \operatorname{area}(F, F) = \operatorname{area}(F, S)$. Further, Theorem 1 yields $\operatorname{area}(F, F) = \operatorname{area}(F^*, \tilde{F}^*)$, since replacing S by F in Theorem 1 implies replacing S^* by $\tilde{F}^*$. Alltogether we obtain

$$\operatorname{area}(F^*, S^*) = \operatorname{area}(F, S) = \operatorname{area}(F, F) = \operatorname{area}(F^*, \tilde{F}^*),$$

which yields $\operatorname{area}(F^*, S^* - \tilde{F}^*) = 0$. It is easy to see that the mixed area of two parallel triangles vanishes if and only if at least one of these degenerates to a single point. Now, F^* and $S^* - \tilde{F}^*$ are two parallel triangles with vanishing mixed area. Since F^* is a nondegenerate triangle the triangle $S^* - \tilde{F}^*$ degenerates to a single point which implies $S^* = \tilde{F}^*$. □

Analogous to the case $m = 6$ of Theorem 3 we can give a geometric characterization for the quadrilateral case $m = 4$. Note that the derived polygons $\tilde{F}^*$ and S^* degenerate to two pairs of parallel lines (see Figure 2 right). Here, equality of $\tilde{F}^*$ and S^* up to translation means that the two pairs of parallel lines have the same distance.

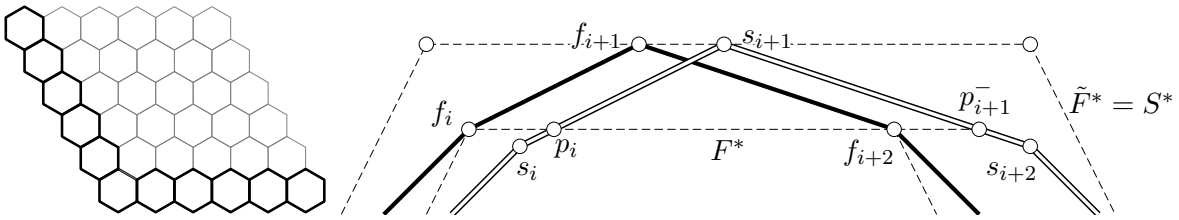

FIGURE 3. *Left:* Schematical image of the discrete Cauchy problem described in 3.1. *Right:* Illustration of a part of two parallel polygons F and S together with their derived polygons F^*, $\tilde{F}^*$ and S^* after an appropriate translation such that $\tilde{F}^* = S^*$. Since $f_i - f_{i+1}$ is parallel to $s_i - s_{i+1}$ it is easy to see that $p_{i+1}^- - p_i = f_{i+2} - f_i$ and $p_i - s_{i+1} = f_i - f_{i+1}$ and $p_{i+1}^- - s_{i+1} = f_{i+2} - f_{i+1}$.

THEOREM 4. *Let $F = (f_0, \dots, f_3)$ and $S = (s_0, \dots, s_3)$ be two parallel quadrilaterals and let $\tilde{F}^*$ and S^* be the derived polygons which degenerate to pairs of parallel lines (see Figure 2 right). Then $H_F = -1$ if and only if S^* and $\tilde{F}^*$ are equal up to translation.*

Proof. The proof is analogous to the hexagonal case (Theorem 3), but with pairs of parallel lines as derived polygons instead of triangles. □

3. Hexagonal meshes as discrete cmc surfaces

We take up Theorem 3 which characterizes pairs of parallel hexagons with $\operatorname{area}(F, F - S) = 0$, or equivalently $H_F = -1$. We derive a construction for a polygon S from a given polygon F such that $H_F = -1$. The other direction i.e., from S to F, seems to be much more complicated and a direct construction is still missing. We can only state another indirect characterization which can be modified into an objective function of a nonlinear optimization problem to generate examples. An illustration of a hexagonal cmc surface which is a discrete surface of revolution can be found in Figure 4.

3.1. **Construction of pairs of hexagons with $H_F = -1$.** Given any hexagon F it is easy to derive a construction from Theorem 3 to generate a quadrilateral S such that $\operatorname{area}(F, F - S) = 0$. We only have to choose three points, say s_1, s_3, s_5 on $\tilde{F}^*$ (we choose the even labeled vertices as derived polygon F^*), draw lines parallel to $f_0 - f_i$, $f_2 - f_i$, and $f_4 - f_i$ through s_i $(i = 1, 3, 5)$ and intersect those lines. Up to translation we obtain a three-parameter family of solutions for S. For an illustration see Figure 2 (left).

This construction can be used to test whether or not a mesh $\mathcal{M}$ is a discrete cmc surface, namely whether or not $\sigma(\mathcal{M})$ exists and approximates a sphere. The existence depends of course on the combinatorics and topology of the mesh but in general we have much more degrees of freedom then in the quadrilateral case (see Section 4). Just by counting degrees of freedom one comes to the conclusion that any hexagonal meshes with regular combinatorics, i.e., like the honeycomb pattern, can serve as Gaussian image of a hexagonal cmc mesh. That is, there is no integrability condition to be fulfilled.

This has an immediate consequence for the following discrete Cauchy problem. Let us assume we are given two strips of parallel hexagons, one arbitrarily lying in $\mathbb{R}^3$ and the other one being part of a hexagonal mesh with honeycomb combinatorics and approximating the sphere, as indicated in Figure 3 (left). Then there is a unique discrete cmc surface containing the first strip.

In the following we are going to derive a statement for arbitrary m-gons (m even) which is a characterization only in the hexagonal case.

Let us assume we are given a pair of parallel m-gons F and S with an even number of vertices and such that the derived polygons S^* and $\tilde{F}^*$ are congruent. Then Theorem 2 yields $\operatorname{area}(F, F-S)=0$. Recall that in the hexagonal case $\operatorname{area}(F, F-S)=0$ implies congruence of S^* and $\tilde{F}^*$ (see Theorem 3). We set

$$\begin{aligned} p_i &:= (f_i + [f_{i+2} - f_i]) \cap (s_i + [s_i - s_{i+1}]),\\ p_i^- &:= (f_{i+1} + [f_{i-1} - f_{i+1}]) \cap (s_i + [s_i - s_{i+1}]), \end{aligned} \tag{7}$$

for i even only. It is now easy to see that

$$\begin{aligned} p_{i+1}^- - p_i &= f_{i+2} - f_i,\\ p_i - s_{i+1} &= f_i - f_{i+1},\\ p_{i+1}^- - s_{i+1} &= f_{i+2} - f_{i+1}, \end{aligned}$$

which is illustrated by Figure 3 (right). This immediately implies the following proposition.

Proposition 5. *Given a polygon S and even labeled points p_i, p_i^-, q_i with*

$$\begin{aligned} &p_i, p_i^- \in s_i + [s_i - s_{i+1}],\\ &q_i = (p_i + [p_i - p_{i+1}^-]) \cap (p_{i-2} + [p_{i-2} - p_{i-1}^-]),\\ &p_i - q_i = p_{i+1}^- - q_{i+2}. \end{aligned}$$

Then there exists a polygon F parallel to S with even labeled vertices $f_i = q_i$ and such that $\operatorname{area}(F, F-S)=0$.

The assumptions of Proposition 5 imply $\tilde{F}^* = S^*$ up to translations and therefore $\operatorname{area}(F, F-S)=0$ (see Theorem 2). Thus, Proposition 5 is an 'if and only if' characterization only for hexagons and quadrilaterals.

4. Quadrilateral meshes as discrete cmc surfaces

At the beginning of this section we focus on a pair of corresponding faces F and $\sigma(F)$ where we are going to use Theorem 4 to derive a construction to obtain a polygon $\sigma(F)$ from a given face F such that $H_F = -1$. Further, we will use these properties to obtain the other and more important direction namely generating F from $\sigma(F)$. Then we draw our attention to entire meshes and present a geometric integrability condition for a mesh being the Gaussian image of a discrete cmc surface. Afterwords we narrow our viewpoint to the setting of circular meshes.

4.1. Construction of pairs of quadrilaterals with $H_F = -1$.

Given any quadrilateral F it is easy to derive a construction form Theorem 4 to generate a quadrilateral S such that $\operatorname{area}(F, F-S)=0$. Let us take the even labeled vertices as derived polygon F^*. Thus, we only have to choose two points s_1 and s_3 on $\tilde{F}^*$, then draw lines parallel to $f_0 - f_i$ and $f_2 - f_i$ through s_i ($i = 1, 3$) and intersect those lines consistently. Up to translation we obtain a one-parameter family of solutions for S. The construction is illustrated by Figure 2 (right).

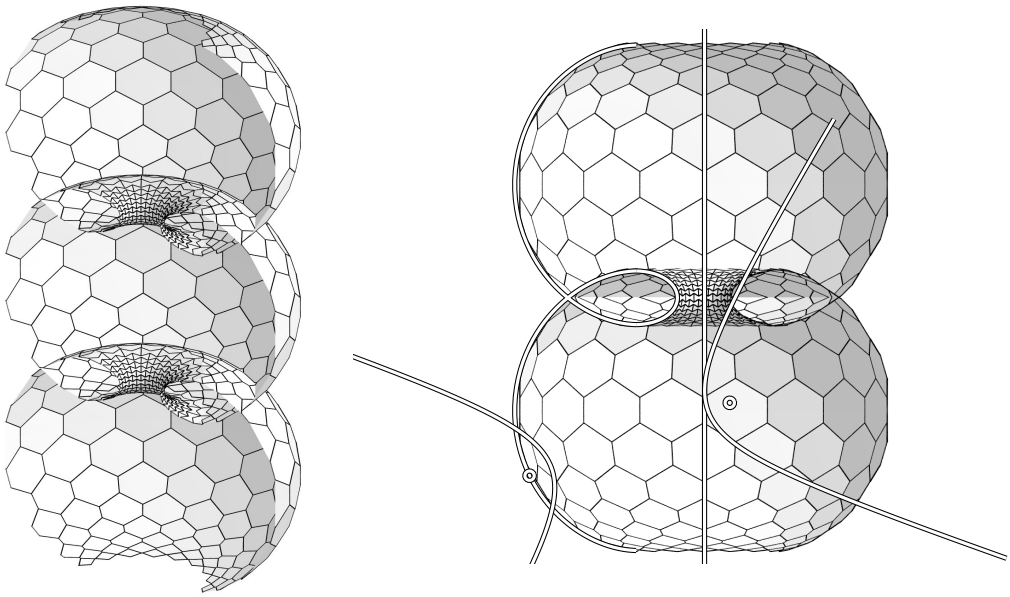

FIGURE 4. A hexagonal cmc surface which discretizes a nodoid. The meridian curve of the smooth nodoid is a so called *nodary* curve which occurs as the locus of a focal point of a hyperbola which rolls along a straight line. In the Figure on the right we can check the meridian polygon of the discretized nodoid against the smooth nodary curve. A visual inspection suggests convergence of the discrete object to its smooth counterpart in an appropriate limit, but a convergence proof is still missing in that setting. For further details on this Figure see Section 6.

Let us recall the meaning of F and S on our discrete surfaces. F represents a face on the discrete surface $\mathcal{M}$ whereas S plays the role of the corresponding face $\sigma(F)$ of the Gaussian image mesh $\sigma(\mathcal{S})$. Thus, the construction described before is only suitable for checking whether or not a mesh $\mathcal{M}$ is a discrete cmc surface. Namely whether or not its Gaussian image $\sigma(\mathcal{M})$ exists and approximates the sphere $\mathbb{S}^2$. We note that the existence of $\sigma(\mathcal{M})$ is equivalent to the integrability of Equation (6) and therefore equivalent to the property of $\mathcal{M}$ being a Koenigs mesh.

To construct F out of S such that $\operatorname{area}(F, F-S) = 0$ might not be so obvious at a first glance. Thus, we need some preparations to obtain such a geometric construction. It is clear from Theorem 4 that in the case of $H_F = -1$ the derived polygons $\tilde{F}^*$ and S^* are equal up to translation as well as $\tilde{F}^{**}$ and S^{**}. Therefore, we can translate the quadrilaterals until $\tilde{F}^*$ equals S^* and $\tilde{F}^{**}$ equals S^{**} as shown in Figure 5. In our translated setting we define

$$p_i := (f_i + [f_i - f_{i+2}]) \cap (s_i + [s_{i-1} - s_i]),$$
$$p_i^- := (f_{i-1} + [f_{i-1} - f_{i+1}]) \cap (s_i + [s_{i-1} - s_i]).$$

Note that the just defined notions vary from those which we defined in (7) for the general (non-quadrilateral) case. We derive from Figure 5 (left) that the triangles f_0, s_0, p_1^- and f_1, p_1, s_1 are congruent which yields $s_0 - p_1^- = p_1 - s_1$. Analogously (Figure 5 right) the triangles f_1, s_1, p_2^- and f_2, s_2, p_2 are congruent which yields $s_1 - p_2^- = p_2 - s_2$. More generally speaking: We have points $p_0, \dots, p_3$ and $p_0^-, \dots, p_3^-$ which fulfill the following

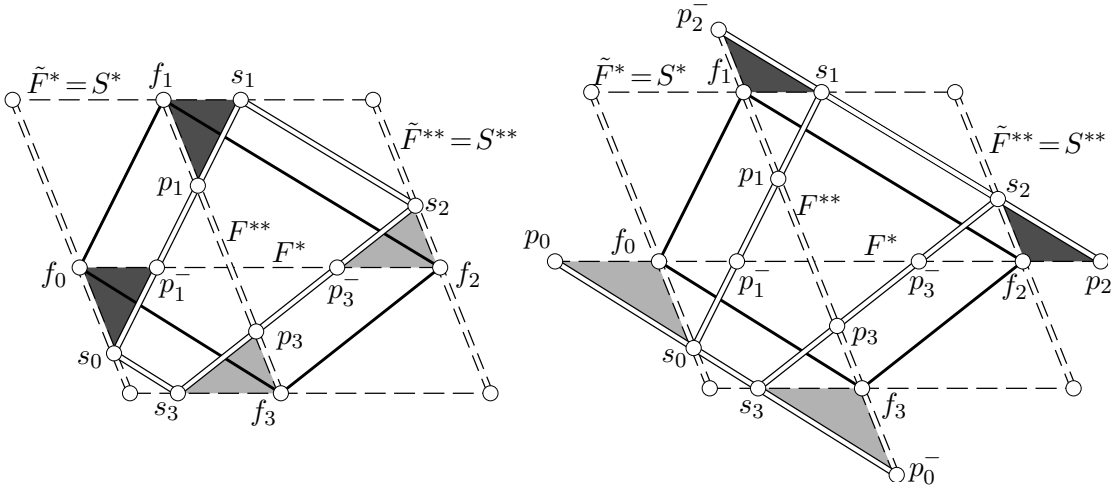

FIGURE 5. We translate the two parallel quadrilaterals $F = (f_0, \dots, f_3)$ and $S = (s_0, \dots, s_1)$ such that the corresponding pairs of derived polygons coincide, i.e., such that $\tilde{F}^*$ coincides with S^* and $\tilde{F}^{**}$ with S^{**}. Thus, equally dashed lines are parallel. We conclude that equally shaded triangles in each figure are congruent triangles which implies $s_0 - p_1^- = p_1 - s_1$ and $f_1 - f_0 = p_1 - s_0$ or more generally (10) and (11).

properties (indices taken modulo 4)

$$p_i, p_i^- \in s_i + [s_{i-1} - s_i], \tag{8}$$

$$\{p_0^-, p_1, p_2^-, p_3\} \text{ and } \{p_0, p_1^-, p_2, p_3^-\} \text{ are collinear, and} \tag{9}$$

$$s_i - p_{i+1}^- = p_{i+1} - s_{i+1} \quad \text{for all } i = 0, \dots, 3. \tag{10}$$

In the following theorem we characterize the configuration of points, lines, incidences and distances given by (8) – (10) in terms of elementary geometry in a more elegant way.

THEOREM 6. *Let $S = (s_0, \dots, s_3)$ be a quadrilateral and let $p_0, \dots, p_3$ and $p_0^-, \dots, p_3^-$ be points lying on respective edges of S as specified by* (8)*. Then property* (10) *is equivalent to the existence of a hyperbola through $s_0, \dots, s_3$ with asymptotes $p_1 + [p_1 - p_3] = p_0^- + [p_0^- - p_2^-]$ and $p_0 + [p_0 - p_2] = p_1^- + [p_1^- - p_3^-]$ as illustrated by Figure 6 (left). The hyperbola can degenerate into a pair of straight lines which then consists of two diagonals of S or a pair of opposite edges.*

Proof. First, we need to recall some properties from elementary geometry about hyperbolas. Let us consider an arbitrary hyperbola together with an arbitrary straight line which intersects the hyperbola in two points A_1, A_2. The points of intersection of the line with the corresponding asymptotes are denoted by B_1, B_2. Then we get $A_1 - B_1 = B_2 - A_2$ (independent from the labeling). Therefore, property (10) follows immediately from the existence of a hyperbola with the described asymptotes.

Conversely, we start with a quadrilateral S such that Equation (10) holds. Again, elementary geometry tells us that there is a unique hyperbola which has two given lines as asymptotes and which passes through one given point. As asymptotes we take $p_1 + [p_1 - p_3]$ and $p_0 + [p_0 - p_2]$ and for the point we take s_0. It is now easy to see that

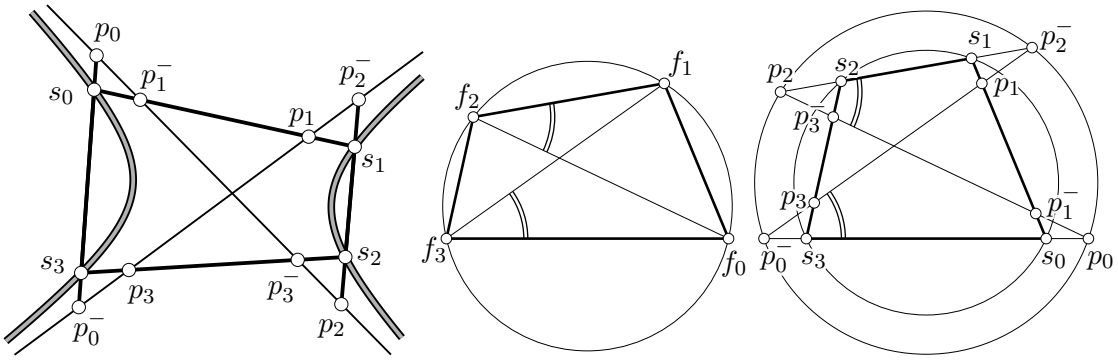

FIGURE 6. *Left:* Illustration of Theorem 6: The vertices of a quadrilateral $S = (s_0, \dots, s_3)$ and points $p_0, \dots, p_3$ and $p_0^-, \dots, p_3^-$ fulfill properties (8) – (10) if and only if there is a hyperbola through the vertices of S and with $p_1 + [p_1 - p_3] = p_0^- + [p_0^- - p_2^-]$ and $p_0 + [p_0 - p_2] = p_1^- + [p_1^- - p_3^-]$ as asymptotes. *Center:* A quadrilateral $F = (f_0, \dots, f_3)$ with a circumcircle. The inscribed angle theorem implies that the marked angles are equal. *Right:* A quadrilateral $S = (s_0, \dots, s_3)$ such that, together with F (center image), we have $\text{area}(F, F - S) = 0$, or equivalently, such that $H_F = -1$. The sides of the corresponding angles which are marked in F and S are pairwise parallel. Thus, the marked angles are equal. Therefore, the inscribed angel theorem implies that the four points p_0, p_0^-, p_2, p_2^- have a circumcircle too.

due to the facts from elementary geometry which we used for the other direction of this proof all the other three vertices s_1, s_2, s_3 have to lie on this hyperbola as well. □

We immediately see that Theorem 6 yields the construction we are looking for, namely to generate F from a given quadrilateral $S = \sigma(F)$ such that $H_F = -1$. We could even do this construction by means of compass and ruler, as we will see. Given a quadrilateral S, we choose an arbitrary direction for one asymptote, i.e., geometrically speaking we choose a point at infinity. The hyperbola through the four points of S and through that point at infinity has two asymptotes which intersect the edges of S in points p_i and p_i^-. With the help of Figure 5 we obtain $p_2^- - f_1 = s_2 - f_2 = p_3 - f_3$ which implies that the diagonal vector $f_1 - f_3$ equals $p_2^- - p_3$ and $p_1 - p_0^-$, and analogously $f_2 - f_0$ equals $p_2 - p_1^-$ and $p_3^- - p_0$. Further, we obtain

$$f_i - f_{i-1} = s_i - p_i^- = p_i - s_{i-1}, \tag{11}$$

i.e., the edges and diagonals of F are already directly determined by S, p_i and p_i^-. Thus, we can easily construct a one parameter family of polygons F such that $\text{area}(F, F - S) = 0$ or equivalently $H_F = -1$.

4.2. **Integrability condition for Gaussian images of cmc surfaces.** We come back to the question for which meshes $\mathcal{S}$ we could get a discrete cmc surface $\mathcal{M}$ with $\sigma(\mathcal{M}) = \mathcal{S}$. In other words, which meshes $\mathcal{S}$ are suitable for Gaussian image meshes of a discrete cmc surface. We already encountered an algebraic characterization with Equation (6): There exists a discrete cmc surface $\mathcal{M}$ with faces F to a given Gaussian image mesh $\mathcal{S}$ with faces S if and only if there exists a real-valued function ν defined on the vertices of $\mathcal{S}$ such that Equation (6) holds for all pairs of corresponding faces.

The following theorem presents the equivalent geometric version of this integrability condition. It answers the question which meshes $\mathcal{S}$ together with points p_i and p_i^-

permit the transformation (11) from $\mathcal{S}$ to $\mathcal{M}$, i.e., from the discrete Gaussian image to the corresponding discrete cmc surface.

THEOREM 7 (Geometric integrability condition). *Let $\mathcal{S}$ be a quadrilateral mesh, i.e., with the combinatorics of a quad-graph $\mathcal{G}$, and such that $\mathcal{S}$ approximates a part of a sphere. Then each of the following statements is equivalent to the others.*

(i) *$\mathcal{S}$ is the Gaussian image mesh of a discrete cmc surface.*
(ii) *There exists a real-valued function $\nu : V(\mathcal{G}) \to \mathbb{R} \setminus 0$, i.e., defined on the vertices, such that the difference equation* (6) *is integrable.*
(iii) *For all pairs S_1, S_2 of adjacent faces of $\mathcal{S}$ the associated points p_i, p_i^- of S_1 and S_2 which fulfill properties* (8) – (10) *coincide on the common edge.*
(iv) *For all faces S of the mesh $\mathcal{S}$ there is a hyperbola going through all four vertices with the following property: For adjacent faces the corresponding asymptotes are intersecting on the common edge, as illustrated by Figure 7.*

Proof. Statement (ii) is just a rewriting of (i) into the setting of Christoffel duality. For details see [4, Section 4.5]. The equivalence of (iii) and (iv) follows directly from Theorem 6.
(i) $\Rightarrow$ (iii): There is a discrete cmc surface $\mathcal{M}$ whose corresponding Gaussian image is $\mathcal{S}$. Therefore, there exist points p_i and p_i^- for each face S fulfilling properties (10) and (11). I.e., $p_i = s_{i-1} + f_i - f_{i-1}$ and $p_i^- = s_i - f_i + f_{i-1}$. We conclude that those pairs of points p_i, p_i^- only depend on those vertices of S and F which lie on the common edge. Thus, p_i, p_i^- are independent of the exact face they are assigned to. That is why those points coincide on common edges which yields (iii).
(iii) $\Rightarrow$ (i): For each face S of $\mathcal{S}$ we use the transformation (11) to obtain a face F. Since corresponding points p_i and p_i^- on common edges of adjacent faces coincide we obtain the same edge length from (11) for their common edge no matter which face we use for computation. Therefore, the so generated faces close up to a discrete cmc surface $\mathcal{M}$ which implies (i). □

REMARK 8. *We would like to mention here that Theorem 7 is still true if $\mathcal{S}$ does not approximate a sphere. However, a discrete constant mean curvature surface with respect to some arbitrary Gaussian image would take us too far away from the smooth setting.*

4.3. **Circular cmc meshes.** Discrete Gaussian images can be understood as polyhedral surfaces approximating the sphere. Thus, one of the natural ways to define such a Gaussian image is as a polyhedral surface inscribed to the unit sphere, i.e., where all vertices are contained in the sphere. In the quadrilateral case this requirement implies two things. First, all faces of all parallel meshes have a circumcircle and second, all parallel meshes possess vertex offset meshes (see e.g., [11, 16]). Those meshes are called *circular* meshes. It turns out that in the circular mesh case our discrete cmc surfaces are discrete isothermic surfaces, as introduced in [2] and extensively studied with respect to discrete cmc surfaces in [6, 8]. In [8] the 'loop group method' is used to obtain cmc surfaces from discrete holomorphic functions. The approach in [6] is via Christoffel- and Darboux transformations with the following main result. A discrete isothermic net $\mathcal{M}$ is cmc (with mean curvature H) if and only if there is a Christoffel transform $\mathcal{M}^*$ of

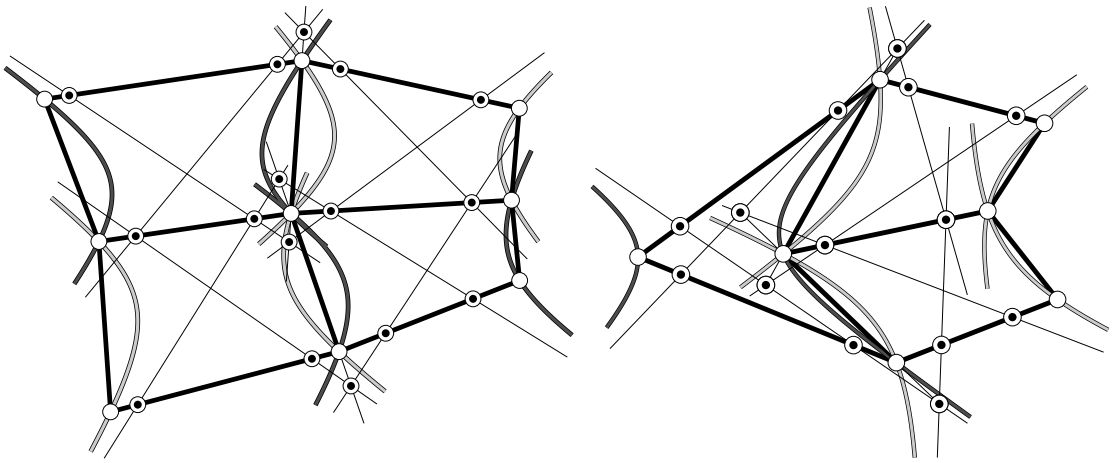

FIGURE 7. Illustration of the geometric integrability condition of Theorem 7 for quadrilateral meshes. Four quadrilaterals around one vertex on the left hand side and three quadrilaterals around one vertex on the right hand side. The vertices of each quadrilateral are lying on a hyperbola. The integrability condition is fulfilled if and only if the asymptotes of the hyperbolas corresponding to adjacent faces are intersecting on the common edge. Such meshes $\mathcal{S}$ can serve as discrete Gaussian images of a discrete cmc surface $\mathcal{M}$, i.e., $\sigma(\mathcal{M}) = \mathcal{S}$.

$\mathcal{M}$ at constant distance, i.e., $\|f_i - f_i^*\|^2 = 1/H^2$ for all pairs of corresponding vertices $f_i \in \mathcal{M}$ and $f_i^* \in \mathcal{M}^*$.

In the following we are looking at discrete Gaussian images of cmc surfaces and obtain the following geometric characterization.

PROPOSITION 9. *Let S be a quadrilateral with a circumcircle and let $p_0, \dots, p_3$ and $p_0^-, \dots, p_3^-$ be points fulfilling* (8) *and* (9)*. Then the following are equivalent.*

(i) *$p_0, \dots, p_3$ and $p_0^-, \dots, p_3^-$ fulfill* (10)*, i.e., $s_i - p_{i+1}^- = p_{i+1} - s_{i+1}$.*
(ii) *Each of the two quadrilaterals p_1^-, p_1, p_3^-, p_3 and p_0, p_2^-, p_2, p_0^- has a circumcircle, and all three occurring circles have the same center.*

Proof. (i) $\Rightarrow$ (ii): First, we construct F, up to translation, with formula (11). F is a quadrilateral which is parallel to S. Elementary counting of angles in a quadrilateral implies that for two edge wise parallel quadrilaterals either both have a circumcircle or none of them. Hence, since S has a circumcircle so does F. The diagonals of F have directions $p_1 - p_3$ and $p_1^- - p_3^-$. The inscribed angle theorem implies that the two angles $\angle(f_2 - f_1, p_3^- - p_1^-)$ and $\angle(f_3 - f_0, p_3 - p_1)$ are equal (see Figure 6 center and right). The same angles appear for $\angle(p_2 - p_2^-, p_2 - p_0)$ and $\angle(p_0^- - p_0, p_0^- - p_2^-)$, which yields the existence of a circumcircle for p_0, p_2^-, p_2, p_0^-. The center of the circumcircle of p_0, p_2^-, p_2, p_0^- lies on the perpendicular bisectors of $p_0 p_0^-$ and $p_2 p_2^-$ which are the same as the perpendicular bisectors of $s_0 s_3$ and $s_1 s_2$, respectively, since (10) has to be fulfilled. Analogously, we can show the same for p_1^-, p_1, p_3^-, p_3.
(ii) $\Rightarrow$ (i): We have to show (10). This is obvious because of the existence of concentric circles, one containing s_i, s_{i+1} and the other one containing p_{i+1}, p_{i+1}^- (see Figure 6 right). $\square$

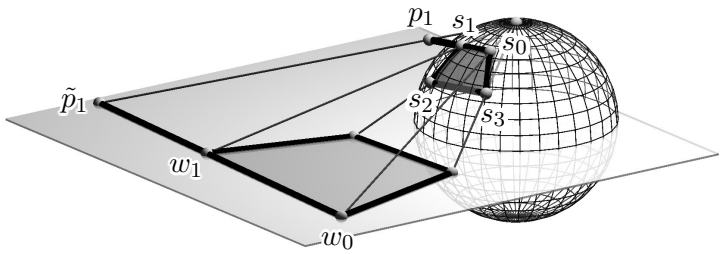

FIGURE 8. The stereographic projection of a quadrilateral $S = (s_0, \dots, s_3)$ from the sphere to the quadrilateral $(w_0, \dots, w_3)$ in $\mathbb{C}$. p_1 is being projected to $\tilde{p}_1 = \lambda_1 w_0 + (1-\lambda_1)w_1$. This λ_1 plays a role in the Weierstrass type representation for discrete cmc surfaces, see Theorem 11.

5. A discrete Weierstrass type representation for discrete cmc surfaces

The classical *Weierstrass representation* formula is a parametrization of minimal surfaces and establishes a bijective relation between minimal surfaces and holomorphic functions. As references see e.g., [5, 12].

In time the Weierstrass representation has been generalized in many aspects. One of these generalizations has been made by K. Kenmotsu [9, 10] to describe cmc surfaces. In contrast to the classical Weierstrass representation, Kenmotsu's version establishes a bijective relation between cmc surfaces and harmonic maps on the sphere. A map n to the sphere is *harmonic*, if $\Delta n \perp T_n\mathbb{S}^2$ where Δ is the Laplace operator. Equivalently, after applying the stereographic projection p, we obtain harmonicity of $w := p \circ n$ if and only if

$$w_{z\overline{z}} - \frac{2\overline{w}}{1+|w|^2} w_z w_{\overline{z}} = 0, \tag{12}$$

where $z = x+iy$ and where w_z, $w_{\overline{z}}$ denote Wirtinger's derivatives, i.e., $w_z = \frac{1}{2}(\frac{\partial w}{\partial x} - i\frac{\partial w}{\partial y})$, and $w_{\overline{z}} = \frac{1}{2}(\frac{\partial w}{\partial x} + i\frac{\partial w}{\partial y})$. K. Kenmotsu [10] proved the following theorem.

THEOREM 10 (Weierstrass type representation for cmc surfaces). *Let $f : U \subset \mathbb{C} \to \mathbb{R}^3$ be a conformal parametrization and for any function $w : U \to \mathbb{C}$ and $H = const. \neq 0$ we set*

$$\psi := \frac{-2}{H} \cdot \frac{1}{(1+|w|^2)^2} \cdot \overline{w}_z.$$

Then f is a cmc surfaces with constant mean curvature H if and only if w is a harmonic function, i.e., w fulfills (12)*, and*

$$f(z) = \operatorname{Re} \int_0^z \psi(1-w^2, i(1+w^2), 2w)\, d\zeta.$$

Then, w is the stereographic projection of the Gauss map of f.

5.1. **Discrete Weierstrass type representation for cmc surfaces.** The aim of the present paragraph is to discretize the smooth Weierstrass type representation from Theorem 10. The idea is similar to the discretization of the classical Weierstrass representation for discrete minimal surfaces in the setting of discrete isothermic surfaces by A.I. Bobenko and U. Pinkall [2].

We start with a quadrilateral mesh $\mathcal{S}$ whose vertices are contained in the unit sphere $\mathbb{S}^2$ and which fulfills the equivalent conditions of Theorem 7. Consequently, $\mathcal{S}$ is the Gaussian image mesh of a circular cmc surface $\mathcal{M}$. Further, Theorem 7 implies that any mesh $\mathcal{S}$ which is the Gaussian image of a discrete cmc surface comes with points p_k and p_k^- on each edge fulfilling (8) – (10). Now we use indices labeled by k instead of i not to get confused with the complex number $i = \sqrt{-1}$. The stereographic projection maps the vertices s_k of $\mathcal{S}$ to vertices w_k of a mesh $\mathcal{W}$ contained in $\mathbb{C}$. The central projection which extends the same stereographic projection to the three dimensional real projective space maps p_k from the line spanned by $s_{k-1}s_k$ to a point $\tilde{p}_k$ on the line spanned by $w_{k-1}w_k$, see also Figure 8. Thus, $\tilde{p}_k$ is an affine combination of w_{k-1} and w_k

$$\tilde{p}_k = \lambda_k w_{k-1} + (1-\lambda_k) w_k, \tag{13}$$

for some $\lambda_k \in \mathbb{R}$. Note that $\mathcal{W}$ is the stereographic projection of the Gaussian image $\mathcal{S}$ of a cmc surface $\mathcal{M}$. Consequently in analogy to Theorem 10 we can call the mesh $\mathcal{W}$ *discrete harmonic*.

THEOREM 11 (Weierstrass type representation for discrete cmc surfaces). *Let $\mathcal{W}$ be a discrete harmonic, circular mesh with quad-graph combinatorics in $\mathbb{C}$. Further, let $\mathcal{W}$ together with some given points $\tilde{p}_k$ and values λ_k for each edge fulfill Equation* (13). *Then the edge vectors of the corresponding discrete cmc surface $\mathcal{M}$ with constant mean curvature $H \neq 0$ can be expressed by*

$$\delta f_{k-1} = \mathrm{Re}\big[\Psi\,(1 - w_{k-1}w_k,\ i(1 + w_{k-1}w_k),\ w_{k-1} + w_k)\,\big],$$

where

$$\Psi = \frac{-2}{H} \cdot \frac{(1-\lambda_k)}{\lambda_k(1+|w_{k-1}|^2)^2 + (1-\lambda_k)(1+|w_k|^2)(1+|w_{k-1}|^2)} \cdot (\overline{w}_k - \overline{w}_{k-1}).$$

Proof. First, we show the representation formula for $H = -1$. By Equation (4) a scaling of the discrete cmc surface by a factor $1/H$ then yields a discrete cmc surface with constant mean curvature H.

The idea of the proof is as follows. We start with an edge $w_{k-1}w_k$ from $\mathcal{W}$ which carries the point $\tilde{p}_k$

$$\tilde{p}_k = \lambda_k w_{k-1} + (1-\lambda_k) w_k,$$

where λ_k is determined by (13). We have to compute the stereographic projection of w_{k-1} and w_k to the sphere i.e., we get vertices s_{k-1} and s_k of a mesh $\mathcal{S}$ in the unit sphere. We use the corresponding central projection to project $\tilde{p}_k$ to the line spanned by $s_{k-1}s_k$ to get p_k (see Figure 8). Then we easily obtain the edge vectors of our discrete cmc surface we are looking for via

$$\delta f_{k-1} = p_k - s_{k-1},$$

where we used Equation (11).

Let us now move to the computation of δf_{k-1}. We determine p_k as affine combination of s_{k-1} and s_k, i.e., there is a γ_k such that $p_k = \gamma_k s_{k-1} + (1-\gamma_k)s_k$ and therefore $\delta f_{k-1} = (1-\gamma_k)\delta s_{k-1}$. Thus, we compute the central projection of $p_k = \gamma_k s_{k-1} + (1-\gamma_k)s_k$

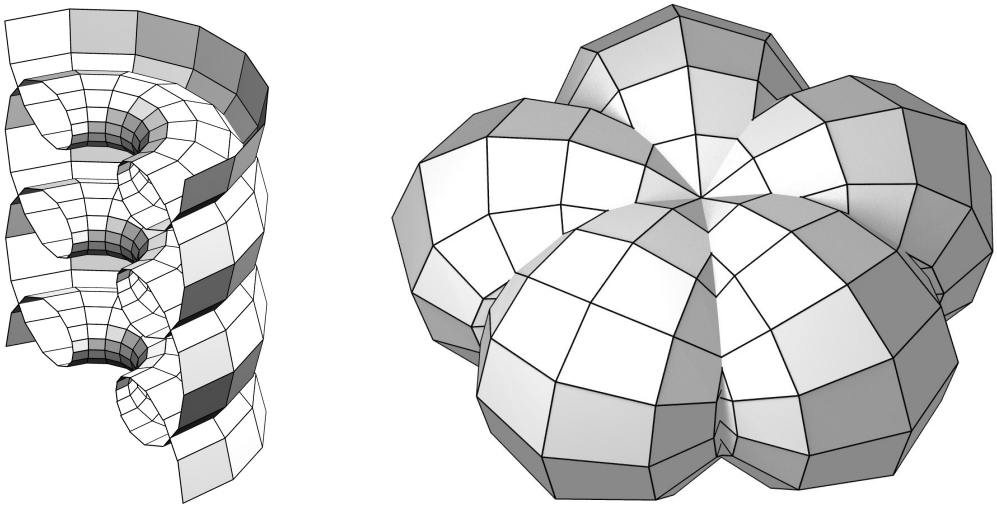

FIGURE 9. A discrete Delaunay surface (left) and a discrete Wente torus (right). For a description and further details see Section 6.

and compare it with $\tilde{p}_k = \lambda_k w_{k-1} + (1-\lambda_k) w_k$. After a lengthy but straightforward computation we obtain for the coefficient γ_k

$$1 - \gamma_k = \frac{(1-\lambda_k)(|w_k|^2+1)}{\lambda_k(|w_{k-1}|^2+1) + (1-\lambda_k)(|w_k|^2+1)}. \tag{14}$$

If we write the stereographic projection as

$$s_k = \Big(\frac{2w_k}{|w_k|^2+1}, \frac{|w_k|^2-1}{|w_k|^2+1}\Big) \in \mathbb{C}\times\mathbb{R} \cong \mathbb{R}^3,$$

we obtain

$$\delta s_{k-1} = \Big(\frac{w_{k-1}(\overline{w}_{k-1}w_k - 1) - w_k(w_{k-1}\overline{w}_k - 1)}{(|w_{k-1}|^2+1)(|w_k|^2+1)}, \frac{|w_k|^2 - |w_{k-1}|^2}{(|w_{k-1}|^2+1)(|w_k|^2+1)}\Big).$$

We compute the real and imaginary part of the first component of δs_{k-1} which correspond to the x and y components of δs_{k-1} as regarded as vector in $\mathbb{R}^3$. Since

$$\begin{aligned}\operatorname{Re}\big(w_{k-1}(\overline{w}_{k-1}w_k - 1) - w_k(w_{k-1}\overline{w}_k - 1)\big) &= \operatorname{Re}\big((\overline{w}_k - \overline{w}_{k-1})(1 - w_{k-1}w_k)\big)\\ \operatorname{Im}\big(w_{k-1}(\overline{w}_{k-1}w_k - 1) - w_k(w_{k-1}\overline{w}_k - 1)\big) &= \operatorname{Re}\big((\overline{w}_k - \overline{w}_{k-1})(w_{k-1} + w_k)\big)\end{aligned}$$

we can write

$$\delta s_{k-1} = \operatorname{Re}\Big[\frac{2(\overline{w}_k - \overline{w}_{k-1})}{(|w_{k-1}|^2+1)(|w_k|^2+1)}(1 - w_{k-1}w_k, i(1+w_{k-1}w_k), w_{k-1}+w_k)\Big].$$

Multiplying the last equation by $1-\gamma_k$ from (14) concludes the proof. □

6. Examples

6.1. **Discrete sphere.** A very simple example of a cmc surface would be a sphere. In the Weierstrass type representation, Theorem 10, the harmonic map $w(z) = -1/\overline{z}$ and

the constant $H = 1$ lead to the rational parametrization

$$f(x+iy) = \Big(\frac{2x}{x^2+y^2+1}, \frac{2y}{x^2+y^2+1}, \frac{x^2+y^2-1}{x^2+y^2+1}\Big) \tag{15}$$

of the unit sphere. In the discrete analogue, Theorem 11, the discrete harmonic mesh $\mathcal{W}$ with $\mathbb{Z}^2$ combinatorics is given by vertices $w_{m,n} = -1/(m-in)$. For 'λ_k' we use the notation $\lambda^m_{m,n}$ for the edge $w_{m-1,n}w_{m,n}$ and $\lambda^n_{m,n}$ for the edge $w_{m,n-1}w_{m,n}$. We set $\lambda^m_{m,n} = \lambda^n_{m,n} = 0$ for all m, n. Replacing w_{k-1} by $w_{m,n-1}$ and w_k by $w_{m,n}$ we obtain

$$\Psi = \frac{-2(\overline{w}_{m,n} - \overline{w}_{m,n-1})}{(1+|w_{m,n}|^2)(1+|w_{m,n-1}|^2)} = \frac{2(m-2mn+i(n^2-n-m^2))}{(1+m^2+n^2)(2+m^2-2n+n^2)},$$

and further

$$\text{`}\delta f_{k-1}\text{'} = f_{m,n} - f_{m,n-1} = f(m+in) - f(m+i(n-1)),$$

with $f(\cdot)$ from Equation (15). I.e., the difference vectors δf_{k-1} correspond to difference vectors of the parameter lines of the smooth parametrization f of the unit sphere. Further, if we choose $f_{0,0} = (0,0,-1)$ as initial value for the integration of the difference equation of Theorem 11, we obtain $f_{m,n} = f(m+in)$ as discrete parametrization of the unit sphere.

6.2. **Discrete cylinder.** Another simple example of a cmc surface is a cylinder. For $w(x+iy) = \cos(x) + i\sin(x)$ and $H = 1$ we obtain the parametrization

$$f(x+iy) = \Big(\sin^2\frac{x}{2}, -\frac{\sin x}{2}, -\frac{y}{2}\Big)$$

of the cylinder with equation $(x-1/2)^2 + y^2 = 1/4$. The Gaussian image of a cylinder is just the great circle. In the discrete setting we take a strip of congruent rectangles around the equator as discrete Gaussian image mesh. We therefore construct a mesh $\mathcal{W}$ with $\mathbb{Z}^2$ combinatorics as follows. Let $c > 1$, $\varphi > 0$, and

$$w_{m,n} = \begin{cases} c\exp(im\varphi) & \text{for even } n, \\ \frac{1}{c}\exp(im\varphi) & \text{for odd } n. \end{cases}$$

Further, let

$$\lambda^n_{m,n} = \begin{cases} 0 & \text{for even } n, \\ \frac{-2}{c^2-2} & \text{for odd } n. \end{cases}$$

and $\lambda^m_{m,n} = 0$ for all m, n. First, we consider an edge defined by vertices with indices $(m, n-1)$ and (m, n) where n is even. Then $\lambda_k = \lambda^n_{m,n} = 0$, $w_{k-1} = w_{m,n-1} = \exp(im\varphi)/c$, $w_k = w_{m,n} = c\exp(im\varphi)$, and

$$\Psi = \frac{2c(c^2-1)\exp(-im\varphi)}{(1+c^2)^2} \quad \text{and} \quad f_{m,n} - f_{m,n-1} = \Big(0, 0, \frac{2-2c^2}{1+c^2}\Big),$$

which is a vector parallel to the z axis and independent of m. Next, we consider an edge defined by vertices with indices $(m, n-1)$ and (m, n) where n is odd. Then $\lambda_k = \lambda^n_{m,n} = -2/(c^2-2)$, $w_{k-1} = w_{m,n-1} = c\exp(im\varphi)$, $w_k = w_{m,n} = \exp(im\varphi)/c$, which yields the exact same Ψ and difference $f_{m,n} - f_{m,n-1}$ as before. I.e., the discrete

parameter lines in 'n'-direction are straight lines parallel to the z-axis. For the other type of edges namely $(m-1,n)$ and (m,n) we get for arbitrary n

$$f_{m-1,n} - f_{m,n} = \frac{2c}{1-c^2}\Big[\begin{pmatrix} \cos(m-1)\varphi \\ \sin(m-1)\varphi \\ 0 \end{pmatrix} - \begin{pmatrix} \cos m\varphi \\ \sin m\varphi \\ 0 \end{pmatrix} \Big],$$

which are horizontal vectors rotating about φ around the z axis as m increases by 1. We conclude that $f_{m,n}$ is a discrete cylinder of revolution.

6.3. **Discrete nodoid as quadrilateral mesh.** Figure 9 (left) shows a discrete Delaunay surface. Delaunay surfaces are surfaces of revolution with constant mean curvature. The surfaces of revolution which have non vanishing mean curvature are the spheres, cylinders, nodoids and unduloids. The discretization in the picture corresponds to a nodoid. The meridian curve can be seen as a discretization of the locus of the focus of a hyperbola while rolling on a straight line. See also [7] for discrete rotational cmc surfaces. The picture in Figure 9 (left) was constructed rather directly. We start with a regular polygon on a circle and rotate it about an axis through its center. The so generated mesh is our Gaussian image mesh $\mathcal{S}$. We choose a point, say p_0 on one edge s_0s_1 of $\mathcal{S}$ and successively construct all the other points p_i and p_i^- on all faces such that the integrability condition (Theorem 7) for $\mathcal{S}$ being a Gaussian image mesh of a discrete cmc surface is fulfilled. It turns out that for rotational symmetric meshes this is an easy construction.

Figure 4 shows a hexagonal mesh which assumes the shape of a nodoid. We construct this example as follows: We start with a rotational symmetric hexagonal mesh $\mathcal{S}$ with vertices in the sphere and construct a mesh $\mathcal{M}$ parallel to $\mathcal{S}$ minimizing energies with the following goals: Constant mean curvature $H_F = 1$ for all faces of the mesh, fairness of the mesh, and same discrete rotational symmetry as $\mathcal{S}$. The discrete cmc surface which we get discretizes a smooth nodoid but with planar hexagons instead of quadrilaterals. Figure 4 (right) shows in addition a smooth nodary curve and indicates how close the discrete nodoid approximates the smooth one.

6.4. **Discrete Wente torus.** Figure 9 (right) shows a discrete Wente torus. A Wente torus is a compact cmc surface. H. Wente [21] was the first to show the existence of a compact constant mean curvature surface in $\mathbb{R}^3$ which is not a sphere. The picture in Figure 9 (right) is the result of an optimization process because a construction via the discrete Weierstrass type representation is still missing and remains future research.

The initialization mesh of the optimization was constructed with a smooth parametrization of the Wente torus. The optimization process uses objective functions which optimize for planarity of all faces, fairness of the mesh, and the connection (11) with an appropriate Gaussian image mesh.

Acknowledgments

This research was supported by the DFG Collaborative Research Center TRR 109, 'Discretization in Geometry and Dynamics' through grant I 706-N26 of the Austrian Science Fund (FWF).

References

[1] Alexander I. Bobenko, Tim Hoffmann, and Boris Springborn. Minimal surfaces from circle patterns: Geometry from combinatorics. *Ann. of Math.*, 164:231–264, 2006.

[2] Alexander I. Bobenko and Ulrich Pinkall. Discrete isothermic surfaces. *J. Reine Angew. Math.*, 475:187–208, 1996.

[3] Alexander I. Bobenko, Helmut Pottmann, and Johannes Wallner. A curvature theory for discrete surfaces based on mesh parallelity. *Math. Annalen*, 348:1–24, 2010.

[4] Alexander I. Bobenko and Yuri B. Suris. *Discrete differential geometry: Integrable Structure*. Number 98 in Graduate Studies in Math. American Math. Soc., 2008.

[5] Jost-Hinrich Eschenburg and Jürgen Jost. *Differentialgeometrie und Minimalflächen*. Springer-Verlag, Berlin, 2007.

[6] Udo Hertrich-Jeromin, Tim Hoffmann, and Ulrich Pinkall. A discrete version of the Darboux transform for isothermic surfaces. In *Discrete integrable geometry and physics (Vienna, 1996)*, volume 16 of *Oxford Lecture Ser. Math. Appl.*, pages 59–81. Oxford Univ. Press, New York, 1999.

[7] Tim Hoffmann. Discrete rotational cmc surfaces and the elliptic billiard. In Hans-Christian Hege and Konrad Polthier, editors, *Visualization and Mathematics*, pages 117–124. Springer Verlag, Heidelberg, 1998.

[8] Tim Hoffmann. Discrete cmc surfaces and discrete holomorphic maps. In *Discrete integrable geometry and physics (Vienna, 1996)*, volume 16 of *Oxford Lecture Ser. Math. Appl.*, pages 97–112. Oxford Univ. Press, New York, 1999.

[9] Katsuei Kenmotsu. Weierstrass formula for surfaces of prescribed mean curvature. *Math. Ann.*, 245(2):89–99, 1979.

[10] Katsuei Kenmotsu. *Surfaces with constant mean curvature*, volume 221 of *Translations of Mathematical Monographs*. American Mathematical Society, Providence, RI, 2003. Translated from the 2000 Japanese original by Katsuhiro Moriya and revised by the author.

[11] Yang Liu and Wenping Wang. On vertex offsets of polyhedral surfaces. In *Proc. of Advances in Architectural Geometry*, pages 61–64. TU Wien, 2008.

[12] William H. Meeks, III and Joaquín Pérez. The classical theory of minimal surfaces. *Bull. Amer. Math. Soc. (N.S.)*, 48(3):325–407, 2011.

[13] Christian Müller and Johannes Wallner. Oriented mixed area and discrete minimal surfaces. *Discrete Comput. Geom.*, 43:303–320, 2010.

[14] Ulrich Pinkall and Konrad Polthier. Computing discrete minimal surfaces and their conjugates. *Experiment. Math.*, 2:15–36, 1993.

[15] Ulrich Pinkall and Ivan Sterling. On the classification of constant mean curvature tori. *Ann. of Math. (2)*, 130(2):407–451, 1989.

[16] Helmut Pottmann, Yang Liu, Johannes Wallner, Alexander I. Bobenko, and Wenping Wang. Geometry of multi-layer freeform structures for architecture. *ACM Trans. Graphics*, 26(3):#65,1–11, 2007.

[17] Robert Sauer. *Differenzengeometrie*. Springer-Verlag, Berlin, 1970.

[18] W. K. Schief. On the unification of classical and novel integrable surfaces. II. Difference geometry. *R. Soc. Lond. Proc. Ser. A Math. Phys. Eng. Sci.*, 459(2030):373–391, 2003.

[19] W. K. Schief. On a maximum principle for minimal surfaces and their integrable discrete counterparts. *J. Geom. Phys.*, 56(9):1484–1495, 2006.

[20] John M. Sullivan. Curvatures of smooth and discrete surfaces. In *Discrete differential geometry*, volume 38 of *Oberwolfach Semin.*, pages 175–188. Birkhäuser, Basel, 2008.

[21] Henry C. Wente. Counterexample to a conjecture of H. Hopf. *Pacific J. Math.*, 121(1):193–243, 1986.

Institute of Discrete Mathematics and Geometry, Vienna University of Technology. Wiedner Hauptstrasse 8-10/104, 1040 Vienna Email: cmueller@geometrie.tuwien.ac.at